

# Novel Control Schemes Based on Recurrent Fuzzy Neural Networks for the Variable Structure UPFC

Tsao-Tsung Ma, *Member, IEEE*

**Abstract**—In this paper, the operating principles and the unique control features of a variable structure unified power flow controller (VSUPFC) on the basis of its feasible hardware implementations, working modes, advanced control functions and flexibilities under different system operating conditions are firstly investigated. Then, a new control scheme using recurrent fuzzy neural controllers is proposed for the VSUPFC to improve the dynamic control performance of real-time power flow control functions with the aim of reducing the inevitable interactions between the real and reactive power flow control parameters. For the purpose of analysing the coupled dynamics of the VSUPFC and the parameters of the controlled power system model, the equivalent controlled current and voltage sources model is adopted for mathematically modeling the VSUPFC and the test power system. To simplify the theoretical analysis of the control system the three phase description of a test power system embedded with a VSUPFC is transformed into d-q components based on a synchronously rotating reference frame. For the VSUPFC control systems with inherent nonlinear coupling features, a feed-forward control scheme based on fuzzy neural controllers is developed to realize the decoupling control objectives. Based on the simulation results, it has been confirmed that the proposed VSUPFC has a number of advantages over the conventional UPFC with fixed hardware structure. In addition, the FNN based control scheme is able to overcome the drawbacks of the conventional power flow controllers designed on small disturbance linearizing method. Comprehensive simulation results on the EMTDC/PSCAD and MATLAB programs are presented and discussed to verify the effectiveness of the proposed VSUPFC and control schemes.

**Index Terms**—power systems, variable structure unified power flow controller, fuzzy neural networks.

## I. INTRODUCTION

Transmission networks play an important role in power system operations, which form the links between power generations and load centres, are essentially designed for delivering reliable, high quality and low-cost power to users. Their limitations are normally caused by steady-state and dynamic operating conditions. With the trend of open

transmission access, relieving these limitations and improving their controllability is of increasing importance. The concept of Flexible AC Transmission System (FACTS) was first proposed by Dr. N. Hingorani in 1986, in which power electronic devices were utilized to eliminate the limitations in conventional power system control means and to improve the overall system operating performance [1]. Basically, there are various definitions of FACTS given by power engineers and researchers working in this field; however, it can be broadly defined as a power transmission system where high-capacity power electronic devices, advanced control technologies and communication technologies are utilized to improve its transmission reliability, controllability, and efficiency. Over the last decade, a huge amount of research into FACTS has been conducted [2]. Based on the reported research results, it can be concluded that many power system operation benefits, which were not attainable in the past, are now achievable by applying FACTS controllers. This is mainly because that these FACTS controllers can force power to flow on the prescribed transmission routes and allow secure loading of transmission lines up to their thermal limits. In fact, there are a number of FACTS devices which have been working in the real-life power systems for years. These devices include the shunt connected controllers (Static Synchronous Compensator, STATCOM [3], Static Synchronous Generator, SSG [4]), the series connected controllers (Static Synchronous Series Compensator, SSSC [5], Thyristor Controlled Series Capacitor, TCSC [6]) and the Unified Power Flow Controller (UPFC) [7-9], combined both the series and shunt control modules, which has been commonly accepted to be the most powerful and versatile one. The installation of the world's first UPFC has been completed and a series of commissioning tests were conducted at the Inez substation of American Electric Power (AEP) in eastern Kentucky. The project is a collaborative effort between AEP, the Westinghouse Electric Corporation, and the Electric Power Research Institute (EPRI). Comprising two  $\pm 160$  MVA voltage sourced GTO thyristor-based inverters (total inverter rating of  $\pm 320$  MVA), this installation is the first large-scale practical demonstration of the UPFC concept, and its completion is a significant milestone in the progress of power electronics technology for FACTS.

The first part of this paper mainly deals with the investigation of a SPWM based variable structure UPFC (VSUPFC) with

Manuscript received May 30, 2007. This work was supported in part by the National Science Council of Taiwan, R.O.C. under contract: NSC-95-2221-E-239-050.

Tsao-Tsung Ma is with the Department of Electrical Engineering, National United University, Miaoli, 36003, TAIWAN, R.O.C. (phone: 886-37-381369; fax: 886-37-327887; e-mail: tonyma@nuu.edu.tw).

emphasis on the possible benefits and new power flow control features in its different operating modes. The advantages and performances of the VSUPFC as a flexible P and Q controller working on a simplified power transmission system model will be fully investigated through comprehensive computer simulations and the results will be presented and analyzed. In recent years, many researches have been focused on how to operate FACTS controllers to enhance power system stability and achieve better utilization of existing power networks. In the aspect of controller design, a simultaneous control of real and reactive power flow using UPFC based on linear control technique has been reported in [10]. Performing the design tasks in d-q domain, a decoupled control scheme with the internal predictive loop is investigated in [11]. However, most of the reported control schemes are designed on a linearized model of the controlled power system. To achieve robust control effects and better control performances some advanced controllers with adaptive features and somewhat with the ability of learning will be required. It is well known that adaptive control is able to better the control of a nonlinear system with fast changing dynamics, such as a power system. This is as a result of the dynamics being continually identified by a model. In this aspect, fuzzy and neural networks are very suitable for multivariable applications especially for the system with unclear and complex dynamics since they can easily identify the interactions between the system's inputs and outputs. The ability to learn and store information about system nonlinearities allows neural networks to be used for modeling and designing intelligent controllers for power systems [12], [13]. Thus, they offer potential alternatives to those applications where the traditional linear controllers are not working adequately. Advantages of the neural network based controllers over the conventional controllers are that they can adapt to the changes in system operating conditions automatically unlike the conventional controllers whose performances degrade for such changes and are required to be retuned to give the desired performance. In second part of this paper the recurrent fuzzy neural network (RFNN) [14], [15] controllers are designed to achieve a decoupled P-Q control of the VSUPFC series branch in a two-bus test power system. The design of the continually online trained RFNN controllers are based on the direct adaptive control scheme. In this study, two sets of RFNNs are used for the complete VSUPFC series branch control. A comparative study of the performances of the proposed controllers and the conventional PI controllers for real-time power flow regulation is presented and briefly discussed.

II. VSUPFC CONFIGURATIONS AND ITS SERIES BRANCH CONTROLLERS

A. The configuration of a VSUPFC

A UPFC has the flexibility to control either its series branch or shunt branch or both to achieve a desired effect on the power flow transmitted between two buses in which the UPFC is connected. In this section, the development of a Variable Structure Unified Power Flow Controller (VSUPFC), based on the basic UPFC configuration, is further used to provide flexible, simultaneous and real time control of the transmission parameters with a real-time variable control structure and

system ratings. Theoretically there are a number of feasible solid-state implementations of the above mentioned VSUPFC; however, when practical implementation is considered the feasibility of circuit configuration, the control algorithm for a specific operating mode, the availability of high capacity power electronics, and most importantly the economical factors must also be taken into account. For the sake of simplicity, a possible VSUPFC hardware configuration using two set of voltage sourced three-phase inverters modules (n=2) operated from a common DC link capacitor as shown in Fig. 1 has been developed as the prototype of a VSUPFC in this study for investigating the possible control modes, and the derivation of its mathematical models for further studies. The same as a conventional UPFC, a VSUPFC can be treated as a universal power flow controller with its rating and structure variable. Therefore, a VSUPFC has the flexibility to control either its series branches or shunt branches or a combination of them to achieve an optimal effect on power system parameters and the purpose of a cost effective installation.

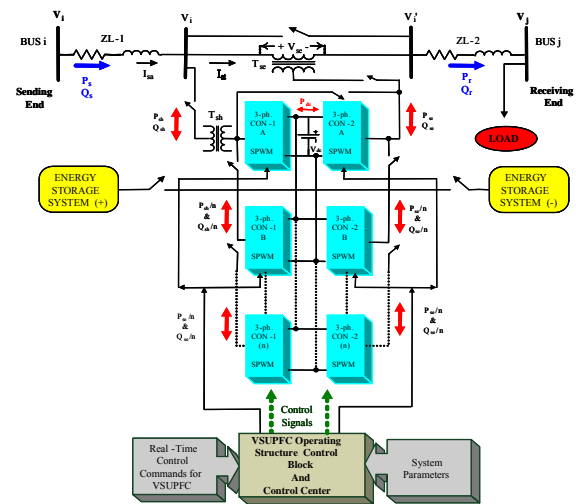


Fig. 1. The basic hardware implementation of a VSUPFC.

For a better understanding of the way that a VSUPFC can be controlled, Fig. 2 gives a conceptual diagram showing the possible controlled quantities of the two branches in a VSUPFC. In order to achieve the purpose of capability transfer between the series and shunt branches of a VSUPFC, it is obvious that a number of small converter modules must be designed for the series and shunt converters.

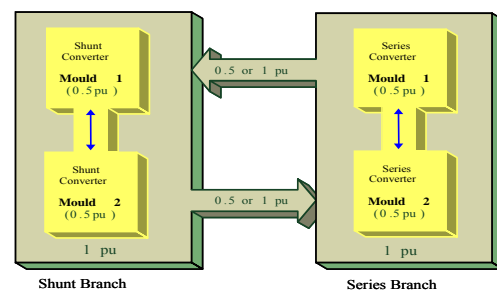


Fig. 2. The capability transfer diagram of a VSUPFC.

Basically, the VSUPFC operating principles and control concepts are the same as that of a UPFC, the basic VSUPFC configuration which consists of two voltage-sourced converters using gate turn off (GTO) thyristor valves (Fig. 1,  $n=2$ ) is chosen to introduce the VSUPFC operating principles. The two converters labelled "CON-1" and "CON-2" in the figure are designed to be operated from a common DC link voltage provided by a common DC storage capacitor. In normal operation, the phase angle of the series voltage can be chosen independently of the phase of line current between 0 and  $2\pi$  and its magnitude can be varied between zero and a pre-specified maximum value. Therefore the active power can freely flow in either direction between the AC terminals of the two converters and each converter can also generate or absorb reactive power independently at its own AC output terminals to affect system voltages. In the VSUPFC system, Converter 2, the series branch, is used to perform the main control functions of a VSUPFC. It generates voltage,  $V_{se}$ , at the system frequency with variable amplitude ( $|V_{se}|$ ) and phase angle ( $\gamma_s$ ) controlled by a proper switching control technique. During the operation, the voltage,  $V_{se}$ , is added to the AC system terminal voltage,  $V_i$ , by the series connected injection transformer,  $T_{se}$ . The shunt converter labelled "CON-1" is operated to draw a controlled current from the bus. One component of this current is automatically determined by the requirement to balance the real power of the series inverter (CON-2). The remaining current component is reactive and can be set to any desired reference level (inductive or capacitive) within the capability of the inverter (CON-1). The reactive compensation control modes of the shunt inverter are very similar to those commonly employed on conventional static var compensators.

B. VSUPFC Control Modes

In practical applications, the VSUPFC control modes are the same as that of UPFC. In the VSUPFC the series converter controls the magnitude and angle of the voltage injected in series with the line. This voltage injection is always intended to influence the flow of power on the line, but the actual value of the injected voltage can be determined in several different ways which are addressed as follows.

- Direct Voltage Injection Mode

In this control mode, the inserted series voltage,  $V_{pq}$ , must be controlled either in phase 0 degrees or in counter phase (180 degrees) with the existing bus voltage,  $V_i$ , and thus changing only the magnitude of  $V_i$ .

- Phase Angle Shifter Emulation Mode

In this control mode, the series convert injects the appropriate voltage so that the voltage,  $V_j$ , is phase shifted

relative to the voltage,  $V_i$ , by an angle specified by reference input.

- Line Impedance Control Emulation Mode

In this control mode, the phase angle of the inserted voltage,  $V_{pq}$ , must be kept at either 90 degrees leading or lagging the transmission line current,  $I$ , to achieve the capacitive or inductive impedance compensation. The series injected voltage is controlled in proportion to the line current so that the series injected voltage appears as an impedance when viewed from the line. The desired impedance is specified by reference input and in general it may be a complex impedance with resistive and reactive components of either polarity. Naturally care must be taken in this mode to avoid values of negative resistance or capacitive reactance that would cause resonance or instability.

- Automatic Power Flow Control Mode

The VSUPFC has the unique capability of independently controlling both the active power flow on a transmission line and the reactive power at a specified value. This capability can be appreciated by interpreting the series injected voltage,  $V_{pq}$ . This injected voltage can be chosen appropriately to force any desired current to flow on the line, hence establishing a corresponding power flow. In automatic power flow control mode, the series injected voltage is determined automatically and continuously by a closed loop control system to ensure that the desired active power and reactive power are maintained despite system changes. The transmission line containing the VSUPFC thus appears to the rest of the power system as a high impedance power source or sink. This is an extremely powerful mode in VSUPFC operations that has not previously been achievable with conventional line compensating equipment. Automatic power flow control can also be used dynamically for power oscillation damping. Fig. 3 shows the effects of active and reactive power exchange between VSUPFC and the controlled power system under different operating conditions.

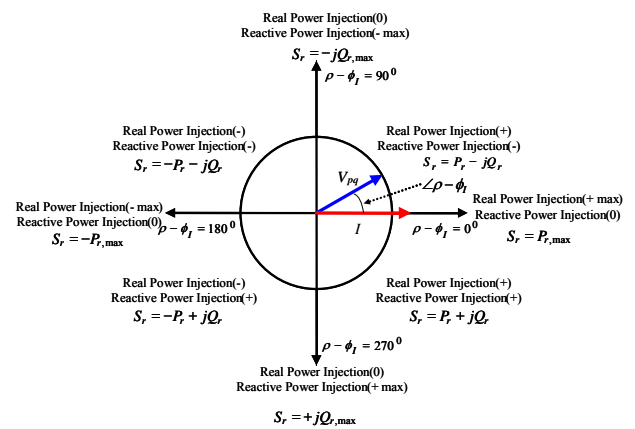


Fig. 3. The active and reactive power exchange between a VSUPFC and the controlled system.

C. Modeling for the series branch controllers

In a VSUPFC system, the series branch provides the main power flow control functions by injecting a voltage with a controllable magnitude and phase angle in series with the line via an insertion transformer. This injected voltage acts essentially like a synchronous ac voltage source. The transmission line current flows through this voltage source resulting in a reactive and active power exchange between itself and the ac system [16]. The basic function of shunt inverter is to generate or absorb the real power demanded by series inverter at the common dc link. The power demand by the series inverter at the dc link is converted back to the ac side of the shunt inverter and fed to the transmission line bus via a shunt-connected transformer. In addition to this, the shunt inverter can also generate or absorb controllable reactive power if desired and thereby provides independent shunt reactive compensation for the system. It is clear that control of real and reactive power on the transmission line can be achieved by injecting series voltage with an appropriate magnitude and angle and the same control theory can also be applied to the controller design of the shunt inverter. For demonstration purposes, only the design procedure of the VSUPFC series branch is presented in this paper.

● VSUPFC Series Branch Controllers

For modelling purposes, the related parameters of the test power system with a VSUPFC are shown in Fig. 4. Based on a preliminary mathematical analysis (small signal analysis) of power flow equations, the P and Q control parameters can be summarized and mathematically expressed as Eq. (4) and (8). Assuming that  $jX_1$  and  $jX_2 \gg R$ , the formulations of P and Q control loops can be easily derived as follows.

$$P_j = \frac{V_j V_R}{X_2} \sin \delta_j ; (\delta_R = 0^\circ) \tag{1}$$

$$dP_j \cong \left( \frac{df}{dV_j} \right) dV_j \tag{2}$$

$$dP_j \cong \left( \frac{d}{dV_j} \left[ \frac{V_{jq} V_R}{X_2} \right] \right) dV_j \tag{3}$$

$$\Delta P_j = \frac{V_R}{X_2} \cdot \Delta V_{jq} \tag{4}$$

$$Q_j = \frac{V_j^2}{X_2} - \frac{V_j V_R}{X_2} \cos \delta_j \tag{5}$$

$$dQ_j \cong \left( \frac{df}{dV_j} \right) dV_j \tag{6}$$

$$dQ_j \cong \left( \frac{d}{dV_j} \left[ \frac{V_j^2}{X_2} - \frac{V_j V_R}{X_2} \cos \delta_j \right] \right) dV_j \tag{7}$$

$$\Delta Q_j = \frac{2V_{jd} - V_R}{X_2} \Delta V_{jd} + \frac{2V_{jq}}{X_2} \Delta V_{jq} \tag{8}$$

By observing Eq. (4) and (8), it is found that the parameters concerning P-Q power flow control loops of the series branch of the VSUPFC is nonlinearly coupled, i.e., the control of real power by adjusting the voltage of  $\Delta V_{jq}$  (Eq. (4)) introduces a coupling term to the reactive power control loop (Eq. (8)). Thus, satisfactory P and Q dynamic control results can only be achieved by using some kind of P-Q decoupled control means. It is clear that the inputs and outputs of the control system in this study case are respectively the power flow control commands and a set of the inverter voltage parameters, i.e., modulation index and phase shift parameters.

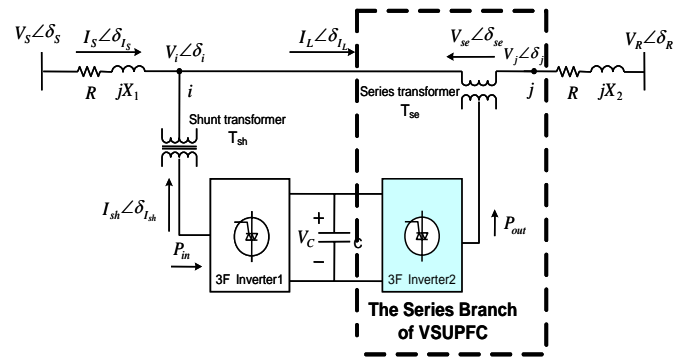


Fig. 4. The test power system with a VSUPFC.

For demonstration purposes, Fig. 5 shows the conceptual control block diagram of the proposed RFNN based and PI controllers for the P-Q decoupled control of the VSUPFC series branch.

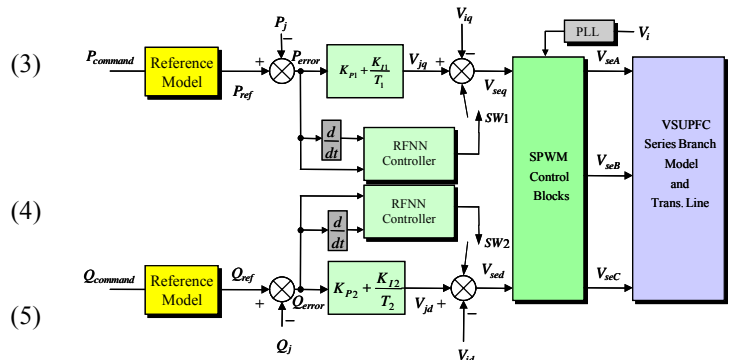


Fig. 5. The conceptual VSUPFC decoupled power flow control scheme with RFNN and PI controllers (series branch).

III. DESIGN OF RECURRENT FUZZY NEURAL NETWORK CONTROLLERS

As stated in the introductory section, in this study two sets of RFNN controllers one for the real power control and the other for the reactive power control of the VSUPFC series branch are used to act as two direct P-Q controllers for decoupling the cross interferences of control parameters and adapting the changing hybrid dynamics of the VSUPFC and the power system conditions.

A. Structure of the RFNN

The structure of a multi-layered RFNN used in this paper is shown in Fig. 6. It has four layers: input layer, membership layer, rule layer, and output layer. In this application case, the RFNN structure is organized into 2 input variables, 3-term nodes for each input variable, 2 output node, and 9 rule and 6 membership nodes. Layer 1 accepts input variables. Its nodes represent input linguistic variables, i.e., Negative (N), Zero (Z) and Positive (P). Layer 2 is chosen as the recurrent layer and used to calculate Gaussian membership values. Nodes in this layer represent the terms of the respective linguistic variables.

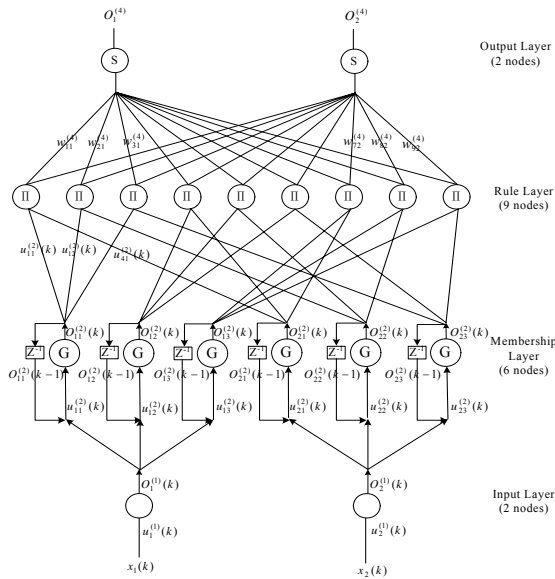


Fig. 6. The multi-layered structure of the proposed RFNN.

Layer 3 forms the fuzzy rule base representing fuzzy rules. Links before layer 3 represent the preconditions of the rules, and the links after layer 3 represent the consequences of the rule nodes. Layer 4 is the output layer, where each node is for an individual output of the system. The links between layer 3 and layer 4 are connected by the weighting values to be on-line trained.

B. Layered operation of the RFNN

To have a clear insight of RFNN principles, this subsection presents the details regarding the signal propagation and the operation functions of the nodes in each RFNN layer. In the

following description,  $u_i^{(k)}$  denotes the  $i$  th input of a node in the layer  $k$ ;  $O_i^{(k)}$  denotes the  $i$  th node output of layer  $k$ .

Layer 1: Input Layer:

The nodes in this layer only transmit input values to the next layer directly, the node input and the node output are represented as

$$\text{node input: } u_i^{(1)} = x_i \tag{9}$$

$$\text{node output: } O_i^{(1)} = u_i^{(1)} \tag{10}$$

where  $i = \{1,2\}$ , From this equation, the link weight at layer 1  $w_i^{(1)}$  is unity.

Layer 2: Membership and Recurrent Layer:

In this layer, each node performs both the membership and recurrent functions. The Gaussian function is adopted here as a membership function.

node input:

$$u_{ij}^{(2)}(k) = O_i^{(1)}(k) + O_{ij}^{(2)}(k-1) \cdot \theta_{ij} \tag{11}$$

$$\text{node output: } O_{ij}^{(2)} = \exp \left\{ - \frac{(O_i^{(1)}(k) + O_{ij}^{(2)}(k-1) \cdot \theta_{ij} - m_{ij})^2}{(\sigma_{ij})^2} \right\} \tag{12}$$

where  $m_{ij}$  and  $\sigma_{ij}$  are the center and the standard deviation of the Gaussian membership function.  $\theta_{ij}$  denotes the link weight of the feedback unit. It can be seen that the input of this layer contains the memory terms,  $O_{ij}^{(2)}(k-1)$ , which store the past information of the network and exhibit an apparent difference between the FNN and the RFNN used here in this paper. Each node in this layer has three adjustable parameters, i.e.,  $m_{ij}$ ,  $\sigma_{ij}$  and  $\theta_{ij}$ .

Layer 3: Rule Layer:

The nodes in this layer are called rule nodes. The following AND operation is applied to each rule node.

$$\text{node input: } u_{ij}^{(3)} = O_{ij}^{(2)} \cdot w_{ij}^{(3)} \tag{13}$$

$$\text{node output: } O_k^{(3)} = \prod_{i=1}^2 u_{ij}^{(3)} \tag{14}$$

where  $k = \{1,2,\dots,9\}$ . The output of a rule node represents the ‘‘firing strength’’ of its corresponding rule. The  $w_{ij}^{(3)}$  is assumed to be unity.

#### Layer 4: Output Layer:

Each node in this layer is called an output linguistic node. The node output is a linear combination of the consequences obtained from each rule. node input:

$$u_q^{(4)} = O_k^{(3)} \cdot w_{kq}^{(4)} \quad (15)$$

$$\text{node output: } O_q^{(4)} = \sum_{k=1}^9 u_q^{(4)} \quad (16)$$

where  $q = \{1, 2\}$ , the link weight  $w_{kq}^{(4)}$  is the output action strength of the  $q$  th output associated with the  $k$  th rule. The  $w_{kq}^{(4)}$  are the tuning factors of this layer, and  $O_1^{(4)} = V_{jd}$  or  $V_{jq}$ ,  $O_2^{(4)} = V_{jq\_com}$  or  $V_{jd\_com}$ .

#### C. On-line Learning Algorithm

To apply the on-line learning algorithm to the proposed RFNN, the gradient descent method is adopted from [11]. Let's take the control of real power as an example, first, the energy function can be defined as:

$$E(k) = \frac{1}{2} (P_{line}^* - P_{line}) = \frac{1}{2} \Delta P_{line}(k)^2 \quad (17)$$

where,  $P_{line}^*$  and  $P_{line}$  represent the real power command and the actual real power in the transmission line ( $P_{ref}$  and  $P_j$  in Fig. 2);  $\Delta P_{line}(k)$  denotes the output error between the real power command and the actual real power. Then, the learning algorithm based on back propagation is described in the following.

Layer 4: The error term to be propagated is given by

$$\delta_q^{(4)} = -\frac{\partial E}{\partial u_q^{(4)}} = -\frac{\partial E}{\partial e} \cdot \frac{\partial e}{\partial P_{line}} \cdot \frac{\partial P_{line}}{\partial O_q^{(4)}} \cdot \frac{\partial O_q^{(4)}}{\partial u_q^{(4)}} \quad (18)$$

and the update rule of  $w_{kq}^{(4)}$

$$w_{kq}^{(4)}(k) = w_{kq}^{(4)}(k-1) + \Delta w_{kq}^{(4)}(k) + \alpha(w_{kq}^{(4)}(k-1) - w_{kq}^{(4)}(k-2)) \quad (19)$$

where,

$$\Delta w_{kq} = -\eta \cdot \frac{\partial E}{\partial w_{kq}} = \eta \cdot \delta_q^{(4)} \cdot u_q^{(4)} \cdot \eta \text{ is the learning rate}$$

of the RFNN weights and  $\alpha$  is the dynamic factor.

Layer 3: Since the weights in this layer are unity, only the error term needs to be calculated and propagated:

$$\delta_k^{(3)} = -\frac{\partial E}{\partial u_k^{(3)}} = -\frac{\partial E}{\partial O_q^{(4)}} \cdot \frac{\partial O_q^{(4)}}{\partial u_q^{(4)}} \cdot \frac{\partial u_q^{(4)}}{\partial O_k^{(3)}} \cdot \frac{\partial O_k^{(3)}}{\partial u_k^{(3)}} = \delta_q^{(4)} w_{kq}^{(4)} \quad (20)$$

Layer 2: The multiplication operation is done in this layer. The error term is computed as follows:

$$\begin{aligned} \delta_j^{(2)} &= -\frac{\partial E}{\partial u_{ij}^{(2)}} \\ &= -\frac{\partial E}{\partial O_q^{(4)}} \cdot \frac{\partial O_q^{(4)}}{\partial u_q^{(4)}} \cdot \frac{\partial u_q^{(4)}}{\partial O_k^{(3)}} \cdot \frac{\partial O_k^{(3)}}{\partial u_k^{(3)}} \cdot \frac{\partial u_k^{(3)}}{\partial O_{ij}^{(2)}} \cdot \frac{\partial O_{ij}^{(2)}}{\partial u_{ij}^{(2)}} \\ &= \sum_k \delta_k^{(3)} O_k^{(3)} \end{aligned} \quad (21)$$

Similarly, the update laws of  $m_{ij}$ ,  $\sigma_{ij}$  and  $\theta_{ij}$  are expressed as follows.

$$m_{ij}(k) = m_{ij}(k-1) + \Delta m_{ij} + \alpha(m_{ij}(k-1) - m_{ij}(k-2)) \quad (22)$$

$$\sigma_{ij}(k) = \sigma_{ij}(k-1) + \Delta \sigma_{ij} + \alpha(\sigma_{ij}(k-1) - \sigma_{ij}(k-2)) \quad (23)$$

$$\theta_{ij}(k) = \theta_{ij}(k-1) + \Delta \theta_{ij} + \alpha(\theta_{ij}(k-1) - \theta_{ij}(k-2)) \quad (24)$$

where,

$$\begin{aligned} \Delta m_{ij} &= -\eta_m \frac{\partial E}{\partial m_{ij}} = -\eta_m \frac{\partial E}{\partial O_{ij}^{(2)}} \cdot \frac{\partial O_{ij}^{(2)}}{\partial u_{ij}^{(2)}} \cdot \frac{\partial u_{ij}^{(2)}}{\partial m_{ij}} \\ &= \eta_m \delta_m^{(2)} \frac{2(x_i^2 + O_{ij}^2(k-1) \cdot \theta_{ij} - m_{ij})}{(\sigma_{ij})^2} \end{aligned} \quad (25)$$

$$\begin{aligned} \Delta \sigma_{ij} &= -\eta_\sigma \frac{\partial E}{\partial \sigma_{ij}} = -\eta_\sigma \frac{\partial E}{\partial O_{ij}^{(2)}} \cdot \frac{\partial O_{ij}^{(2)}}{\partial u_{ij}^{(2)}} \cdot \frac{\partial u_{ij}^{(2)}}{\partial \sigma_{ij}} \\ &= \eta_\sigma \delta_\sigma^{(2)} \frac{2(x_i^2 + O_{ij}^2(k-1) \cdot \theta_{ij} - m_{ij})^2}{(\sigma_{ij})^3} \end{aligned} \quad (26)$$

$$\begin{aligned} \Delta \theta_{ij} &= -\eta_\theta \frac{\partial E}{\partial \theta_{ij}} = -\eta_\theta \frac{\partial E}{\partial O_{ij}^{(2)}} \cdot \frac{\partial O_{ij}^{(2)}}{\partial u_{ij}^{(2)}} \cdot \frac{\partial u_{ij}^{(2)}}{\partial \theta_{ij}} \\ &= \eta_\theta \delta_\theta^{(2)} \frac{-2(x_i^2 + O_{ij}^2(k-1) \cdot \theta_{ij} - m_{ij}) \cdot O_{ij}^2(k-1)}{(\sigma_{ij})^3} \end{aligned} \quad (27)$$

$\eta_m$ ,  $\eta_\sigma$  and  $\eta_\theta$  are respectively the learning-rate parameters for the mean value, the standard deviation of the Gaussian functions and the linking weight of the feedback units in the RFNN.

## IV. CASE STUDIES AND SIMULATION RESULTS

### A. Feasibility studies on VSUPFC

The test power system shown in Fig. 1 is used for computer simulation studies carried out in this section. The initial states of

the test power system are recorded as follows: The generator voltage: 230KV  $\angle 80^\circ$ , system frequency: 60 Hz, line impedance:  $ZL-1+ZL-2=5.29+j52.9 \Omega$ . The VSUPFC shunt transformer is Y-D connected and rated at 100MVA, 230kV/23kV, with a leakage reactance of 10%. The series transformer is connected and rated at 100MVA, 230kV/23kV, with a leakage reactance of 10%. The DC link capacitor is  $4000\mu F$  and its voltage is 43kV. In order to evaluate the capability of the shunt branch of the VSUPFC in supporting the system voltage, a set of PSCAD/EMTDC simulation studies concerning the voltage control effectiveness in a fault case has been carried out. In this study, the fault case is a 3 phase short circuit and the fault resistance is  $10\Omega$ . Fig. 7 and Fig. 8 show the system bus voltage in per unit value (A phase) from 1.95 seconds to 2.9 seconds with and without VSUPFC respectively. Obviously, without the VSUPFC control, the system voltage drops to 0.39 pu during the fault interval. When a VSUPFC is in operation, the bus voltage can be greatly improved as shown in Fig. 8 to Fig. 11. These shows that the VSUPFC shunt converter can produce the reactive power fast enough to support the system bus voltage.

On the simulation results, Fig. 8 and 9 show a set of simulation results concerning the voltage and P-Q control capabilities of VSUPFC with the rating of a single shunt converter case, the system bus voltage can be improved to 0.9 pu during a fault. When the series converter capacity is fully transferred to the shunt converter and the shunt converter capacity becomes double. This enables the shunt branch of VSUPFC to have better voltage control capability. The controlled results are shown in Fig. 10 and 11. As can be seen in Fig. 10, when the shunt converter rating is doubled, the system bus voltage can be improved up to 0.956 pu. Fig. 8 shows the corresponding changes of reactive power.

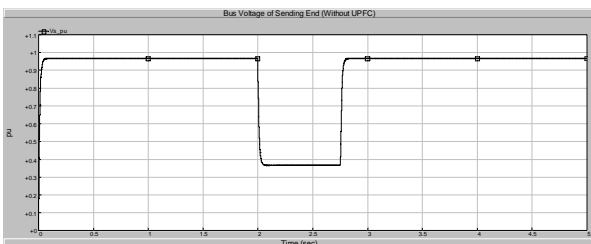


Fig. 7. The bus voltage without the VSUPFC control.

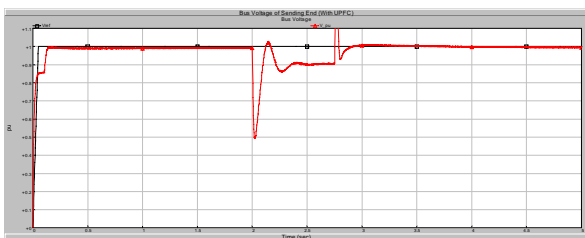


Fig. 8. The improved bus voltage with a VSUPFC in operation (a single shunt converter).

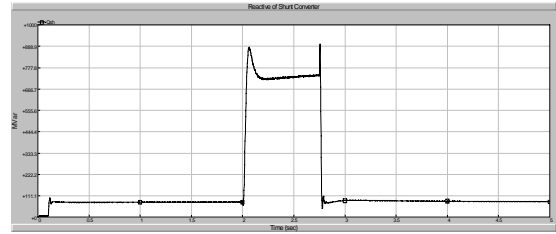


Fig. 9. The changes of output reactive power of the VSUPFC (a single shunt converter).

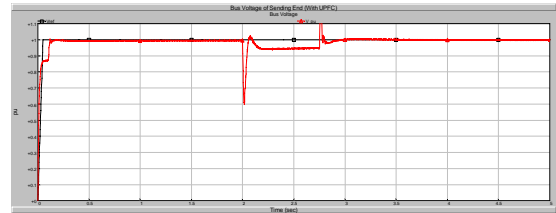


Fig. 10. The improved system bus voltage with a VSUPFC in operation (double shunt converters).



Fig. 11. The changes of output reactive power of the VSUPFC (double shunt converters).

For the power flow control using VSUPFC series branch, when the capacity of series converter is enhanced the range of controllable power flow are enhanced accordingly. In this study, the simulation results for various control modes as addressed previously are investigated. Fig. 12(a) and 12(b) show the P-Q plan and P-Q 3-D figure of control range of VSUPFC series converter as operated in direct voltage control mode respectively. Fig. 13(a) and 13(b) show the same contents of VSUPFC series converter operated in phase shifting mode. Fig. 14(a) and 14(b) show the control results of VSUPFC series converter operated in line impedance regulating mode. Fig. 15 shows the attainable power flow control region of a VSUPFC.

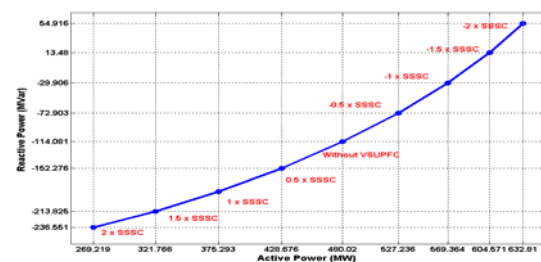


Fig. 12. (a) The P-Q plan of the control range of VSUPFC in direct voltage control mode.

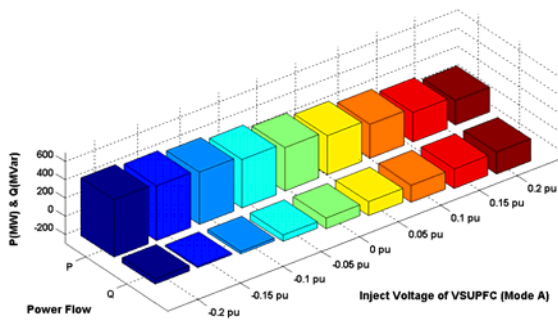


Fig. 12. (b) The P-Q 3D figure of the control range of VSUPFC in direct voltage control mode.

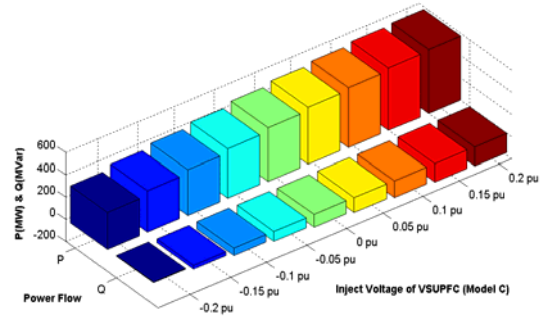


Fig. 14. (b) The P-Q 3D figure of the control range of VSUPFC operated in line impedance regulating mode.

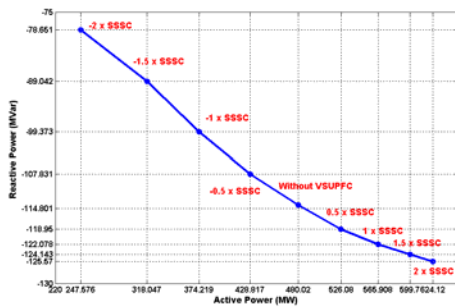


Fig. 13. (a) The P-Q plan of the control range of VSUPFC operated in phase shifting mode.

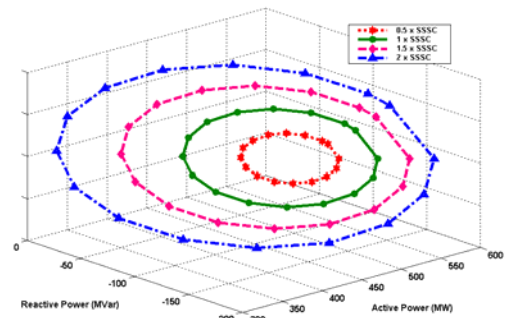


Fig. 15. The attainable power flow control region of a VSUPFC.

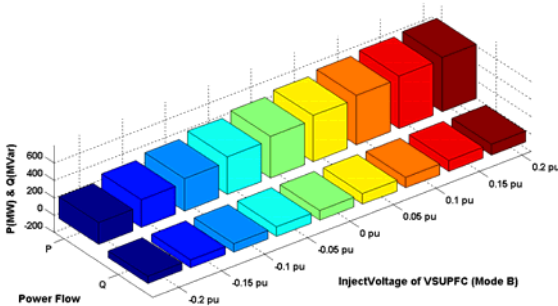


Fig. 13. (b) The P-Q 3D figure of the control range of VSUPFC operated in phase shifting mode.

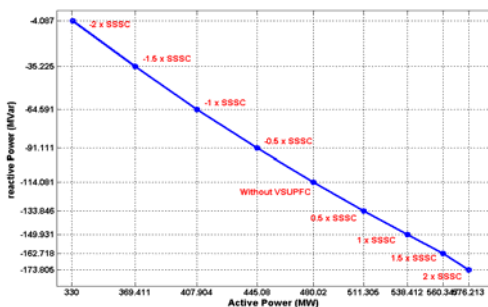


Fig. 14. (a) The P-Q plan of the control range of VSUPFC operated in line impedance regulating mode.

*B. Dynamic power flow control on FNN based VSUPFC*

For identifying the detailed dynamics of the VSUPFC, the two-bus power system embedded with a VSUPFC as shown in Fig. 1 is simulated in a PSCAD/EMTDC environment while the FNN controllers are implemented in a MATLAB program module. PSCAD/EMTDC is an electromagnetic transient simulator for complex electric networks with the capability of modeling power electronics, controls and nonlinear power networks. It also has a flexible interface for exchanging parameters with other simulation programs. The power system in Fig. 1 comprises two buses (two synchronous generators with conventional speed and voltage regulators). The two buses of the test system are connected by two sections of standard transmission lines. The VSUPFC is placed between the two sections of the transmission lines. For simulation purposes, the test system with a nominal voltage of 230KV and a system base of 600MVA is chosen to evaluate the dynamic power flow control performances of the RFNN controlled VSUPFC with two different control schemes, i.e. conventional PI controllers without considering the coupling effects of controlled parameters and the proposed RFNN based direct decoupled control method. Based on the base values of the test system, only the real and reactive power flow control functions, which are performed by the series branch of the VSUPFC, are presented in this subsection. Fig. 16 to Fig. 19 show a set of comparative simulation results. In Fig. 16 to Fig. 19, the curves labelled "A" show the power flow control commands (real or reactive power), while the curves labelled "B" display the



corresponding controlled power flow. It can be clear seen from the simulation results, the proposed RFNN controllers are able to control the VSUPFC much better than the conventional PI controllers in a real-time P-Q control mode. The superior performance of the new approach over the conventional PI controllers can be explained as a result of the online, non-stop learning of the controlled dynamics and the operating conditions of the system by the designed RFNN.

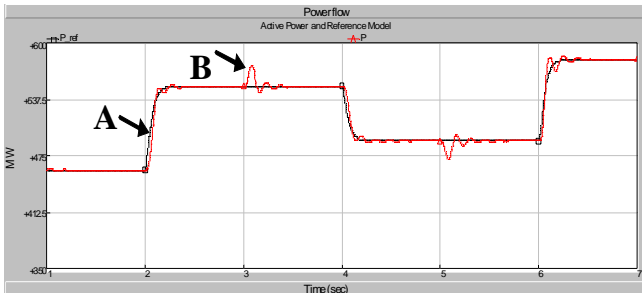


Fig. 16. (a) The results of controlled real power and its control command (two steps up and one step down) using conventional PI controllers (A: control command, B: actual result).

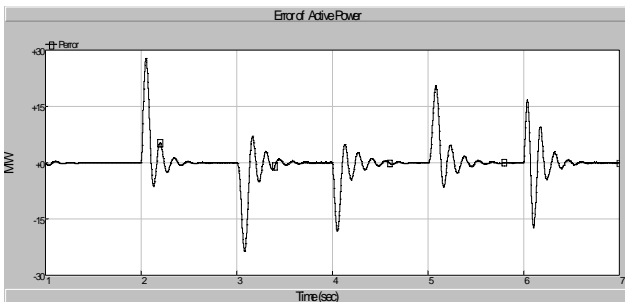


Fig. 16. (b) The calculated control error of real power using conventional PI controllers.

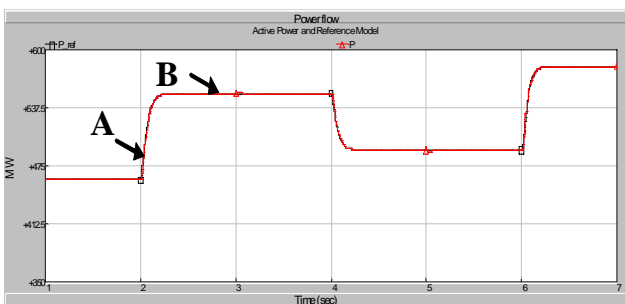


Fig. 17. (a) The results of controlled real power and its control command (two steps up and one step down) using RFNN based direct controllers with decoupling design (A: control command, B: actual result).

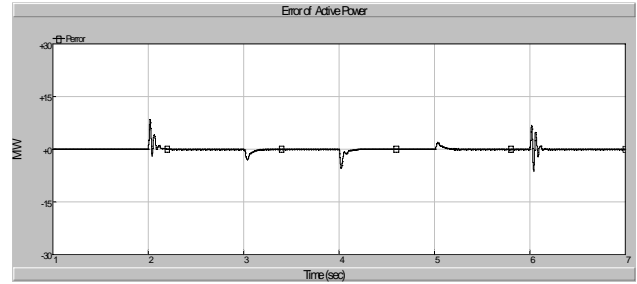


Fig. 17. (b) The calculated control error of real power using RFNN based direct controllers.

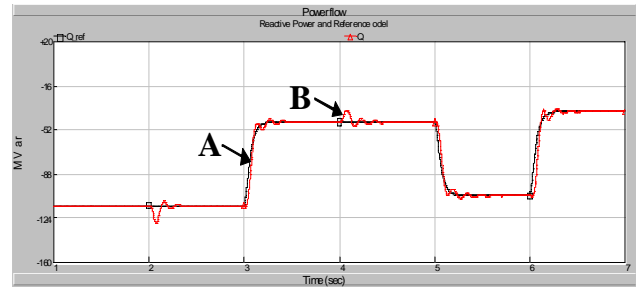


Fig. 18. (a) The results of controlled reactive power and its control command (one step down and two steps up) using conventional PI controllers (A: control command, B: actual result).



Fig. 18. (b) The calculated control error of reactive power using conventional PI controllers.

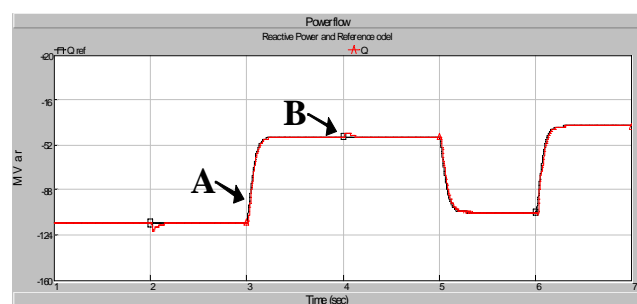


Fig. 19. (a) The results of controlled reactive power and its control command (one step down and two steps up) using RFNN based direct controllers with decoupling design (A: control command, B: actual result).

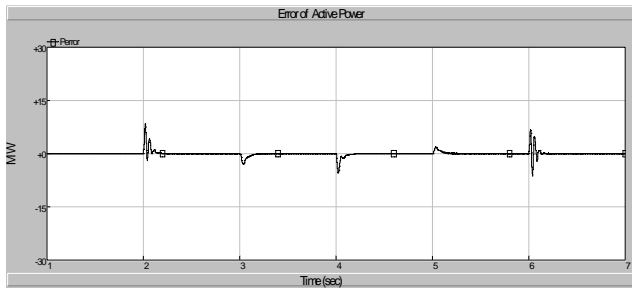


Fig. 19. (b) The calculated control error of reactive power using RFNN based direct controllers.

## V. CONCLUSION

In this paper, the feasibility and dynamic power flow control performance of a VSUPFC are numerically investigated. The special hardware arrangement of two sets of synchronous voltage source converters, one in shunt connection and the other in series connection, has resulted in the unique control flexibility of the VSUPFC system. This particular configuration provides the possibility of performing a concurrent or selectable voltage, impedance, and phase angle regulation. It is important to note that with the proposed VSUPFC configuration, ratings and internal parameters selected for operations can be changed on a real-time basis and without any hardware alterations. In the aspect of controller design, the procedure of mathematical modelling a simple power system embedded with a VSUPFC and the design of a new RFNN based decoupled control scheme for the VSUPFC to improve the dynamic P-Q control performance have been presented. Two continually online trained RFNN controllers are designed to provide adaptive, decoupled control of the VSUPFC series inverters according to the real and reactive power flow control commands. Based on the simulation results, the proposed control scheme can overcome the inevitable instability problems of conventional PI based controllers which are designed on small disturbance linearising method especially when the operating point of the controlled power system changes greatly. It has been shown in this paper that two separate RFNN online-trained controllers are able to successfully adapt themselves to the hybrid complex dynamics of a VSUPFC and the power system over a variety of control modes and a wide range of system operating conditions.

## REFERENCES

- [1] Narain G. Hingorani, "Flexible AC transmission", IEEE Spectrum, April 1993, pp. 40-45.
- [2] A-A. Edris, "Proposed terms and definitions for flexible ac transmission systems (FACTS)", IEEE Trans. on Power Delivery, Vol. 12, No. 4, Oct. 1997, pp. 1848-1853.
- [3] K.V. Patil, J. Senthil, J. Jiang, and R.M. Mathur, "Application of STATCOM for damping torsional oscillations in series compensated ac systems", IEEE Trans. on Energy Conversion, Vol. 13, No. 3, Sept. 1998, pp. 237-243.
- [4] A.A. Edris, "Technology development of flexible ac transmission systems", Proceedings of ICEE'96, pp. 882-888.
- [5] K. K. Sen, "SSSC-static synchronous series compensator: theory, modelling, and applications", IEEE Trans. on Power Delivery, Vol. 13, No. 1, Jan. 1998, pp. 241-246.
- [6] A. Claudio and Z.T. Faur, "Analysis of SVC and TCSC controllers in voltage collapse", IEEE Trans. on Power Systems, Vol. 12, No. 4, Nov. 1997, pp. 1619-1625.
- [7] L. Gyugyi, C.D. Schauder, S. L. Williams, T.R. Rietman, D.R. Torgerson, and A. Edris, "The unified power flow controller: a new approach to power transmission control", IEEE Trans. on Power Delivery, Vol. 10, No. 2, April 1995, pp. 1085-1093.
- [8] A. N. Niaki, and M. R. Iravani, "Steady-state and dynamic models of unified power flow controller (UPFC) for power system studies," IEEE Trans. on Power Systems, Vol. 11, Issue 4, Nov. 1996, pp. 1937-1943.
- [9] T. T. Ma and Kai-Hung Lu, "Performance Analysis of a Variable Structure Unified Power Flow Controller Using PSCAD/EMTDC Transients Simulation Program", The proceedings of ICSS2005, International Conference on Signal and Systems, pp. 145-150.
- [10] K.R.Padiyar, K.Uma Rao, "Modeling and Control of Unified Power Flow Controller for Transient Stability," International journal of Electrical power & Energy Systems, Vol.3, pp. 1-11, 1999
- [11] P. Zunko, D. Povh, M. Weinhold, "Basic Control of Unified Power Flow Controller," IEEE Trans. on Power Systems, Vol. 12, No. 4, Nov.1997pp.1734-1739.
- [12] Schauder CD, HamaiDM, Edris A, et al., "Operation of the Unified Power Flow Controller (UPFC) Under Practical Constraints," IEEE Trans on Power Delivery, 13(2), 1998, pp.630-639.
- [13] K. S. Narendra and K. Parthasarathy, "Identification and control of dynamical system using neural networks," IEEE Trans. Neural Networks, vol. 1, Mar. 1990, pp. 4-27.
- [14] G.K. Venayagamoorthy, R.G. Harley, "A continually online trained neurocontroller for excitation and turbine control of a turbo generator," IEEE Trans. on Energy Conversion, vol.16, no.3, September 2001, pp. 261-269.
- [15] Y. C.Wang, C. J. Chien, and C. C. Teng, "Takagi-Sugeno recurrent fuzzy neural networks for identification and control of dynamic systems," Proceedings IEEE Int. Conf. Fuzzy Systems, Melbourne, Australia, 2001, pp. 537-540.
- [16] K.L. Lo, T.T. Ma, J. Trecat, M. Crappe, "Detailed Real-Time Simulation and Performance Analysis of UPFC Using Electromagnetic Transients Program (EMTP)," Proceedings of POWERCON '98, Beijing, China, August 1998, pp. 889-894
- [17] Leu, Y.G., Lee, T.T., and Wang, W.Y.: 'On-line tuning of fuzzy-neural network for adaptive control of nonlinear dynamical systems', IEEE Trans. Syst. Man Cybern., 1997, 27, pp. 1034-1043.